Acta Cryst. (1995). D**51**, 207–219

Growth Processes of Protein Crystals Revealed by Laser Michelson Interferometry Investigation

BY PETER G. VEKILOV,* MITSUO ATAKA† AND TATSUO KATSURA

National Institute of Bioscience and Human-Technology, 1-1 Higashi, Tsukuba, 305 Japan

(*Received* 9 *August* 1993; *accepted* 21 *June* 1994)

Abstract

The elementary processes of protein crystal growth were investigated by means of laser Michelson interferometry on the example of the (101) face of tetragonal hen egg-white (HEW) lysozyme. The method allows real-time *in situ* observations of the morphology of the growing protein crystal surface, as well as simultaneous precise measurement of growth rate and step velocity on identified growth-layer sources. At the critical supersaturation of 1.6 the growth mechanism was shown to transform from dislocation-layer generation to surface nucleation. Measurements on different growth hillocks, with material of a different source and at a different temperature, all indicated that for supersaturations lower than ~ 1 growth is hindered by the competitive adsorption of (most probably) other protein species contained in HEW, although the material is pure by most analytical methods. At supersaturations $\sigma \leq 0.4$ other impurities sometimes led to cessation of growth. However, at σ in the range $0.9 \leq \sigma \leq 1.6$ growth processes are determined by the kinetics of pure lysozyme. This enabled us to measure the step kinetic coefficient β for crystallization of a protein substance for the first time: $\beta = 2.8\ \mu m\ s^{-1}$. This also means that by working in this supersaturation range we can eliminate the impurity effects. Other means to reduce influence of impurities is to use, if possible, a higher crystallization temperature. It is shown that slow crystallization of proteins is due primarily to impedance of the elementary act of entering the growth site and not to the low concentration of the solution. The value of β does not depend on temperature, indicating the decisive role of entropy, not energy barriers, in the crystallization of biological macromolecules.

1. Introduction

The precise knowledge of the structure of biological macromolecules forms the basis of understanding their function and their mechanism of action (Michel, 1990). The bottleneck of the structure determination by means of X-ray or neutron diffraction now appears to be crystallization, *i.e.* obtaining sufficiently large and perfect crystals of the substance studied (DeLucas & Bugg, 1987; Deisenhofer, 1992). The trial-and-error method to find the best growth mode is still largely applied here (McPherson, 1990, 1992). Two systematic approaches to accelerate the search for optimal crystallization conditions were proposed: The first, the 'incomplete factorial method' (Carter & Carter, 1979; Carter, 1990), provides a recipe of how to estimate the role of numerous factors in the crystallization of the investigated species with considerably few trials. The other approach, initiated by Kam *et al.* (1978), aims at understanding the processes of nucleation and crystal growth at a molecular level by studying the growth kinetics of some model protein (usually hen egg-white lysozyme) and hence to compress the time and the region in which the 'right' crystallization conditions will be sought for each separate case. Furthermore, investigations on nucleation and crystal growth were carried out separately, the former mainly by means of light-scattering techniques (Mikol *et al.*, 1990, Malkin *et al.*, 1992), the latter by measuring the kinetics of growth of protein crystals based on their size and by judging the elementary growth mechanism (Fiddis *et al.*, 1979; Durbin & Feher, 1986). Recently published accurate morphological observations and surface-feature measurements, carried out *ex situ* by electron microscopy (Durbin & Feher, 1990) or *in situ* by means of atomic force microscopy (AFM) (Durbin & Carlson, 1992), provided a deeper insight into the surface processes on the growing protein crystal face. Through these studies it has become increasingly evident that an understanding of crystallization events at the molecular level is the key factor to grow macromolecular crystals in a rational way.

Many of the questions, regarding the molecular processes of protein crystal growth are still without a firm answer. Among these are the relative roles of transport through the solution and surface kinetics; the layer-generation mechanism, dislocation or surface nucleation, and the region of operation of each of them; nature and influence of the uncontrolled impurities in the system; the effect of temperature and the mechanism through which it influences the growth processes. The present paper aims to shed some new light on the problems above by studying the kinetics and morphology on a

* Present address: Center for Microgravity and Materials Research, University of Alabama in Huntsville, Huntsville, Alabama 35899, USA.

† To whom correspondence should be addressed.

growing protein crystal surface. Recently it was shown that a similarity exists between the well known self-assembly processes of G-actin, tubulin, *etc.* and the initial stage (*i.e.* nucleation) of crystal growth of HEW lysozyme (Ataka & Asai, 1990). If such an analogy can also be made regarding the subsequent growth processes, then studying the crystal growth may as well contribute to the understanding of elongation, cessation and dissociation of self-assembling protein molecules.

We chose HEW lysozyme as a crystallizing substance for two main reasons. HEW lysozyme is by far the best studied crystalline protein model. The properties of the crystals and of the solutions (density, refractive index, diffusion coefficient, *etc.*) are known. Numerous investigations of the phase diagrams, growth and related phenomena have been performed and this provides a basis for comparison and verification of our results. The second reason is that a sample of high and controlled purity, to satisfy biochemical standards, is commercially available. All investigations, reported here, were performed on the (101) face of tetragonal HEW lysozyme crystals.

Our method of investigation of the protein crystal growth was laser Michelson interferometry (LMI) (Chernov *et al.*, 1986, Kuznetsov *et al.*, 1987) which has shown its great advantages in studying crystal growth from solution of low molecular weight substances (Rashkovich & Shekunov, 1990*a*; Vekilov *et al.*, 1992*a*; Maiwa *et al.*, 1990). This method allows real-time *in situ* morphological observations and quantitative assessment of various surface features on the growing crystal face (Vekilov *et al.*, 1990). It also enables us to measure very precisely both the normal growth rate and the step velocity on identified growth sources. We recently published a letter on the applicability of LMI to protein crystal growth (Vekilov *et al.*, 1993). Its main disadvantage is the lower vertical resolution compared with AFM: we cannot see separate steps, we need regular step patterns at least 1 μm high, whose average slope can be measured. This limits the application of LMI mostly to dislocation-generated growth, but its advantages are overwhelming.

2. Experimental methods

2.1. *Solutions and seeds*

Solutions were prepared from HEW lysozyme (Seikagaku Kogyo, Tokyo, Lot No. E88Z03 and E92201, 6× crystallized, homogeneous by ultracentrifugal, electrophoretic and chromatographic analysis, containing 1.78%(*w/w*) Cl^-, M_r = 14 307 Da) as received. Some experiments were carried out with HEW lysozyme from a different source (Sigma, 3× crystallized, catalogue No. L-6876, Lot No. 89F8275). A weighed amount of the protein was dissolved in a weighed amount of water purified by reverse osmosis, deionized and subsequently passed through an ultrapure water system (NANOpure, Barnstead). 3.0%(*w/w*) NaCl (Kanto) was added as a precipitant. The pH was adjusted to 4.6 by HCl (Wako) (Ataka & Asai, 1988). The analytically determined concentrations of lysozyme and Cl^- in the solution equalled the weight concentrations (Elgersma *et al.*, 1992).

Seed crystals were grown according to the solubility-gradient method (Ataka & Katsura, 1992) in test tubes held vertically and using $NiCl_2$ as a precipitant. A selected seed, 0.7–1.8 mm, was carefully dragged out of the test tube. In the first experiments, the seed was placed on a glass slide and washed with ~200 μl of lysozyme solution saturated at room temperature, as reported previously (Vekilov *et al.*, 1993). When we later skipped this procedure, we noticed that some of the 'impurity effect' (§3.3) was eliminated. The seed was glued to the crystal holder (Fig. 1). Gluing took about 5 min during which the seed was held in a drop of saturated solution. The holder with the crystal was then inserted into the working solution in the growth cell (Fig. 1). In some experiments etching of the crystal was carried out to obtain a new surface by overheating by 3 K above the temperature at which the seed crystal was grown (295–296 K) for 2–3 h, but this had no effect on the further regeneration and growth of the crystal. Regeneration of the seed crystal was carried out by undercooling by 5 K less than room temperature for 1–2 d. Morphological observations and kinetic measurements were then performed.

2.2. *Experimental set up*

The action of the laser Michelson interferometer is based on the spatial and temporal coherency of the strictly parallel laser beam. After being divided by the beam splitter (STP in Fig. 2), the two parts of the beam are reflected by the surface investigated and the reference

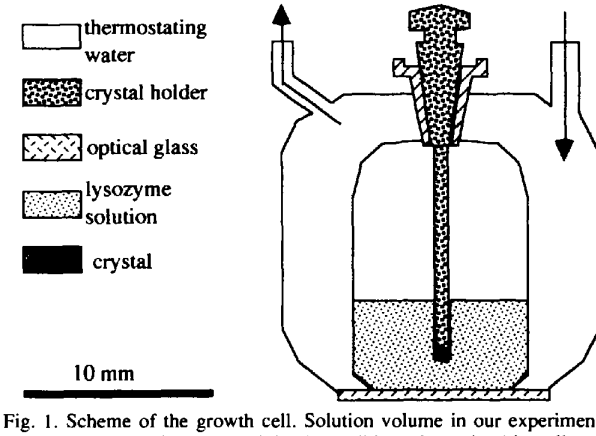

Fig. 1. Scheme of the growth cell. Solution volume in our experiments was 500 or 300 μl, the minimal possible volume in this cell was 200 μl. Temperature was held constant (±0.1 K) in the course of each measurement by connecting the outer volume of the cell to a Haake thermostatic bath.

mirror (M). If some parts of the surface investigated are closer to the beam splitter than others, the portion of the beam reflected by them will have travelled a shorter path, when they return to the beam splitter. Interaction with the reference beam results in an interference pattern, corresponding to the relief on the surface investigated. Places of equal height form one interference fringe and in this way the interference pattern may be regarded as a topographic map of the surface. The scheme of the experimental set up is shown and described in Fig. 2.

2.3. *Observations and measurements*

Each experiment was performed on a separate crystal and denoted *A*, *B*, *etc.*

Because of the very low reflecting ability of the lysozyme crystals and to avoid losing intensity of the laser beam, we did not expand it to the whole width of the studied face. Consequently, we could not observe the whole growing (101) face, but usually 1/4 or 1/3 of it. Before starting measurements the surface was scanned and a part of it, most suitable for observations, was selected. All the following observations and measurements were performed on the same surface features in the course of one experiment. By means of the interferometric table (Fig. 2) the crystal was oriented so that one of the (101) faces was perpendicular to the object laser beam.

Fig. 3 presents a typical interference pattern from the studied face. The difference in height Δ between two neighbouring interference fringes is (Chernov *et al.*, 1986),

$$\Delta = \lambda/2n, \tag{1}$$

where $\lambda = 0.6328$ μm is the wavelength of the laser light, $n = 1.384$ is the refractive index of the working solution, measured for the above wavelength by an Atago refractometer. This value is mainly determined by the NaCl in the solution since lysozyme changes the refractive index of the solution very slightly (Feigelson, 1988). Temperature affects n only negligibly. The value of n of a 3.0wt% aqueous NaCl solution without lysozyme increased only by 0.0016 when the temperature decreased from 290 to 280 K; the same value of a solution containing 3.0wt% NaCl and 2.0wt% lysozyme increased by 0.0020 on going from 298 to 279 K. Thus, we get $\Delta = 0.229$ μm. Note that this is not the height of a single step. By this method we are observing a slope that is formed as a result of the existence of many steps.

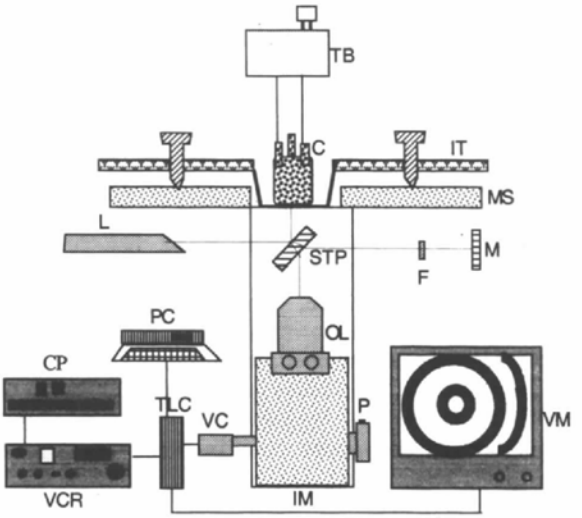

Fig. 2. Scheme of the experimental set up: (TB) thermostatic bath (Haake FK); (C) crystallization cell with the crystal, see Fig. 1 for details; (IT) interferometric table; (MS) microscopic stage; (L) He-Ne laser, $\lambda = 0.6328$ μm, 15 mW (Melles Griot); (STP) semi-transparent plate with chromium coating; (F) filter, 10% transmittance for λ applied; (M) reference mirror; (OL) objective lens (Nikon Plan 5×); (IM) inverted microscope (Nikon Diaphot); (P) photographic camera (Nikon); (VC) CCD colour video camera (Sony); (TLC) time-lapse controller (Sankei SIV-JS); (PC) personal computer (Victor HC-95); (VCR) SuperVHS video cassette recorder (Victor); (CP) colour printer (Mitsubishi SCT-CP 220); (VM) 19″ video colour monitor (Sony Trinitron). The semi-transparent plate reflected 70% of the beam to the growing crystal surface and 30% passed to the mirror. To balance the weak reflection by the protein crystals we had to use the filter (F) for the reference beam. The interference pattern formed at the semi-transparent plate entered the microscope and was transmitted along its optical pathway. The PC-operated time-lapse controller allowed playing of smooth pictures with a great range of acceleration: the minimal interval between recordings was 10 s, the shortest record consisted of three frames. Pictures of interest were printed on the colour printer. LMI is extremely sensitive to vibrations which were avoided by placing the whole set up on an anti-vibration table (Meiritsu AVT 45).

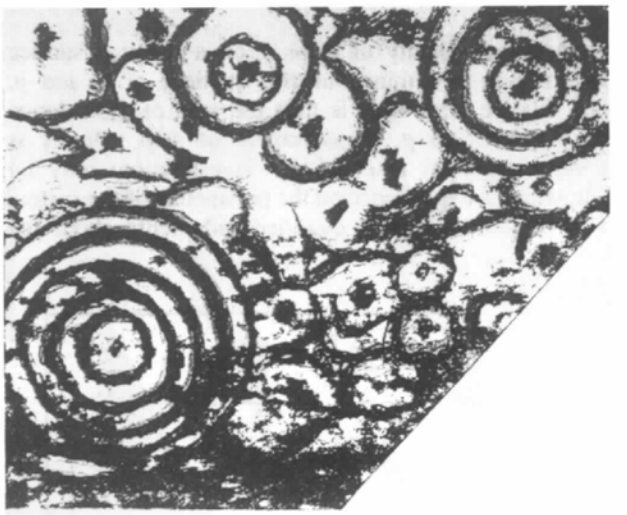

Fig. 3. Typical interference pattern on the (101) lysozyme face (Vekilov *et al.*, 1993). Bar equals 100 μm. The poor quality of the picture is due to the low reflectability of the lysozyme crystals. Approximately 1/4 of the face is shown. The edge with the adjacent (110) face is bottom right. Two major dislocation-growth hillocks, on which measurements could be taken, are bottom left and top right. The surface between them is covered with growth hillocks unsuitable for measurements.

The slope p of the growth hillocks and of other regular patterns on the growing surface was calculated as,

$$p = \Delta/\Delta x, \tag{2}$$

where Δx is the distance between neighbouring fringes on the crystal surface. For experimental points 5–7 such measurements were performed and then the mean value of p and the error limits (as standard deviation) were determined.

When the crystal grows, the interference fringes spread from the centre to the periphery of the growth hillocks. To measure the normal growth rate R of the investigated face from the recorded images we measured 10–20 time intervals, Δt, between fringes passing through a selected point on the slope of the growth hillock. For each Δt the growth rate R was calculated as,

$$R = \Delta/\Delta t. \tag{3}$$

Then the mean value and the error limits of the measurement were calculated as shown in Fig. 4. Usually one measurement took 2–3 h and 10–20 fringes were processed. Several recordings for 8 h showed that R is constant for that time, except for low supersaturations (see below). Thus, the determination of R, carried out so far mostly by following the change in the overall crystal dimensions under a microscope, can now be performed with much higher accuracy and for a known growth-layer source.

Since (Chernov, 1974, 1984, 1989)

$$R = p \cdot \mathbf{v}, \tag{4}$$

the average velocity of steps $\mathbf{v}$ on a selected surface pattern was determined as the quotient of R and p. The relative error of $\mathbf{v}$ is thus the sum of the relative errors of R and p. Measurement of step velocity is a very important asset of our investigation: only by following its dependence on the parameters of the system it is possible to make qualified judgments about the mechanism of incorporation of particles into the crystal and the rate-limiting stages of this process.

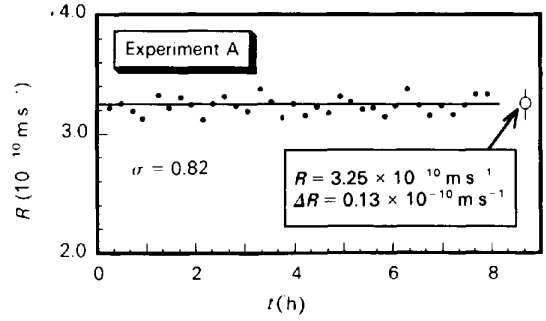

Fig. 4. Measurements of the normal growth rate R for 8 h. Each point corresponds to the passing of one interference fringe. The determination of the mean value and the error interval is illustrated. σ represents supersaturation as defined by (5).

The driving force for crystallization was considered to be thermodynamic supersaturation, measured in kT units ($\Delta\mu/kT$) and denoted as σ. It was imposed by lowering the temperature of the solution and determined as,

$$\sigma \equiv \Delta\mu/kT = \ln[C/S(T)], \tag{5}$$

where C is the actual concentration of the solution in mol l^{-1}, $S(T)$ is the solubility in the same units, determined from the phase diagrams (Ataka & Asai, 1988) as,

$$\ln S = 24.09 - 9100/T, \tag{6}$$

(T is temperature in K).

3. Results

3.1. *Morphological observations*

After regeneration, the crystal surface was usually covered with numerous growth hillocks one or two interference fringes high (~0.4 μm) (the minor growth hillocks in Fig. 3), probably corresponding to dislocations. An X-ray topographic photograph of a lysozyme crystal showed contrasts that are considered to be bundles of broad lines (K. Izumi, private communication); we think that this indicates the presence of dislocations, as opposed to a former hypothesis that dislocations are absent in tetragonal lysozyme crystals (Shaikevitch & Kam, 1981). On average, in one out of two to three experiments we had growth hillocks sufficiently high (five or more interference fringes) for measurements to be performed (the two major growth hillocks in Fig. 3). Fig. 5 shows that the 'suitable' growth hillocks were formed by planar defects outcropping on the surface that can be represented and behave kinetically as dislocation nets (Nanev & Vladikova, 1978; Vekilov & Nanev, 1992). The growth hillocks had the shape of a circular cone and existed for unlimited time in the supersaturation range 0.4–1.6. Even if they disappeared outside this supersaturation interval, on coming back they were formed at the same places. These observations, together with Fig. 5, mean that we are dealing with growth hillocks, generated by dislocations and that the supersaturation range above is the region of operation of the dislocation-growth mechanism.

The slope of the dislocation-growth hillocks remained approximately constant in the course of one experiment. This is natural, since the growth hillocks were generated by planar defects, comprising dislocation nets, which are proved to produce a constant hillock slope in a wide supersaturation range (Vekilov & Nanev, 1992). The p values we obtained on different hillocks and in different experiments were in the range of 1.1×10^2–1.6×10^2.

At supersaturations higher than 1.6 the growth hillocks disappeared. The interference pattern became

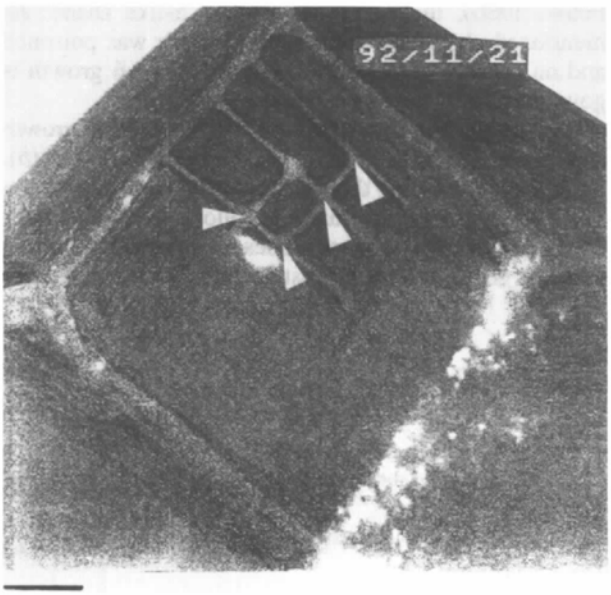

(*a*)

(*b*)

Fig. 5. (*a*) White visible reflected-light picture of the face studied after etching for 1 h by overheating by 3 K. The adjacent dipyramid faces are bottom left and right. The adjacent prism faces are at the top of the picture. Planar defects, presumably induced during the dragging of the seed crystal, are etched at the top part of the face. Illumination comes from the side of the viewer and slightly to the bottom right. (*b*) Interferogram of the top left ~1/4 part of the face in the same experiment as (*a*). The adjacent prism face is top left. Four growth hillocks are formed at the places where the planar defects intersect, marked with arrowheads in (*a*). The formation of a new planar defect can be seen in the centre of the picture, where steps coming from three growth sources meet. Both pictures were recorded on the VCR and then printed on the printer (Fig. 2). Bars in both (*a*) and (*b*) equal 100 μm.

very irregular, the fringes interlaced, moved in all directions, disappeared and appeared again. We believe that this is an explicit evidence that the crystal is growing by the polynucleation mode of the two-dimensional (2D) nucleation mechanism (Weeks & Gilmer, 1979; Chernov, 1984; Malkin *et al.*, 1989). It is generally known that crystals grow by this mechanism at higher supersaturations, and this mechanism was in fact shown to be involved in lysozyme crystal growth (Durbin & Feher, 1986, 1990). We have now managed to determine more precisely the critical supersaturation for the transition from dislocation to 2D nucleation growth for our experimental conditions.

In the first experiments, when the seed crystals had been washed before immersing in the solution, the growth hillocks were gradually lost at $\sigma \leq 0.4$. The surface became rough and did not reflect the laser light. In accordance with the kinetic measurements (see below) we conclude that at these supersaturations the impurities, present in the system, poison the growing surface and growth stops. Further, when we skipped the washing growth proceeded, although with extremely low rates, for supersaturations $\simeq 0.25$ and maybe lower. In some experiments macrosteps (Fig. 6) appeared at $\sigma \simeq 0.4$, but did not appear in the same experiment at lower σ. In other experiments, no formation of macrosteps was observed at any supersaturation. These observations agree with theoretical predictions (Van der Eerden & Müller-Krumbhaar, 1986) that impurity induced macrosteps should appear if both critical supersaturation and critical impurity concentration are reached. On the basis of these facts we conclude that at $\sigma \leq 0.4$ growth is influenced and sometimes stopped by some impurity molecules, the concentration of which depends on preparation.

In one of the experiments (Fig. 7) the interference pattern was broken on the boundary between the growth

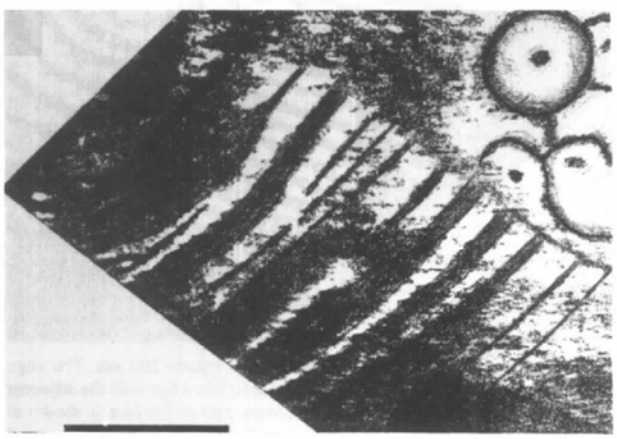

Fig. 6. Macrosteps appearing in experiment *B* at $\sigma = 0.44$, ~6 h after the supersaturation was lowered to this value. Bar equals 100 μm. Edge with adjacent prism face is to the bottom left, while the dipyramid face is to the top left. The macrosteps moved very slowly from the top left to the bottom right. The corresponding decrease in the growth rate is shown in Fig. 9(*b*).

hillocks. Observation in plain light revealed the formation of a cliff, one part of the crystal was growing faster than the other. However, we did not observe steps spreading on the lower crystal surface from the concave angle thus formed. This means that the two parts of the crystal are not crystallographically connected. The two parts have existed from the beginning of the experiment, so this defect probably comes from the seed crystal.

The formation of a planar defect can be seen in Fig. 5(*b*). In this figure four growth hillocks can be seen whose centres coincide with the positions marked with arrowheads in Fig 5(*a*). In the middle of Fig. 5(*b*) three hillocks are encountered where steps from three growth sources meet. We can see that the interference fringes are discontinuous at this position indicating the presence of a step ~0.2 μm high. On the surrounding crystal surface steps spread normally. This defect, characterized by the discontinuous fringes, appeared at high supersaturations and continued to exist until the end of the experiment, but did not increase in size. We assumed that a system of stacking faults or microinclusions was formed at high step velocities in the region of complicated step motion between the three growth hillocks.

3.2. *Dependencies of the normal growth rate and step velocity on supersaturation*

Fig. 8(*a*) presents the dependence of the normal growth rate on the supersaturation in one of the first experiments, denoted *A*. The values are approximately five times higher than those reported earlier (Durbin & Feher, 1986), the curve has a clear *S*-like shape. As mentioned above, for $\sigma \leq 0.4$ the surface was poisoned and no growth was observed, and for $\sigma \geq 1.6$ growth is governed by two-dimensional nucleation.

The reason for this behaviour of the normal growth rate becomes evident from the $v(\sigma)$ plot in Fig. 8(*b*). After the 'dead zone' there is a linear dependence of the step velocity on supersaturation, followed by a fast non-linear increase and a second linear region, extrapolating to the origin. Such characteristic dependencies have been observed in potassium dihydrogen phosphate (KDP)

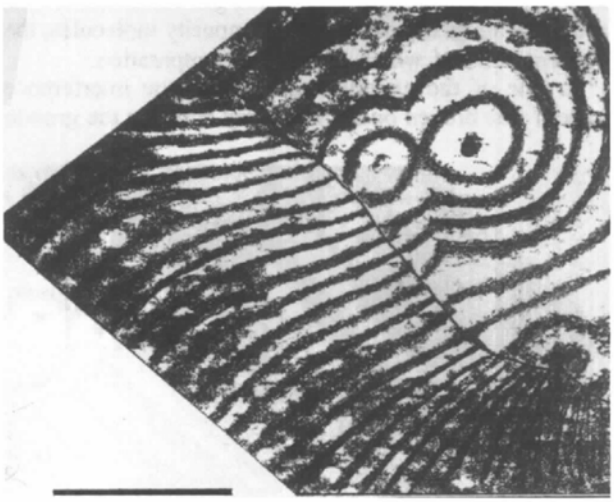

Fig. 7. Interference pattern for crystal *B*. Bar equals 100 μm. The edge with the adjacent dipyramid face is top left. The edge with the adjacent prism face is at the bottom left. The same part of the face is shown at low supersaturation in Fig. 6. The growth hillocks to the right existed for a short time, disappeared at higher supersaturations and did not appear anymore, their part of the surface was occupied by minor hillocks (see Fig. 6). The step pattern at the lower part was probably generated by a strong dislocation source at top left and existed at all supersaturations. The boundary between the two parts of the crystal is seen.

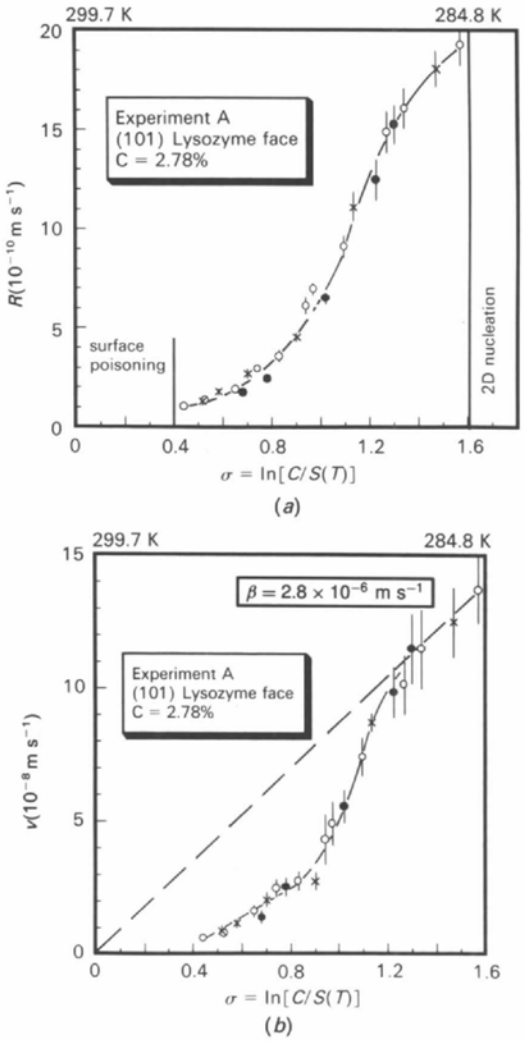

Fig. 8. Kinetic curves measured in experiment *A*. Before immersing into the solution, the seed crystal was washed (§2.1). Different points indicate measurements taken in three series of supersaturation increase, on three subsequent days. On the upper σ axis the temperature interval of the measurements is indicated. Lysozyme concentration in the solution is indicated in the label. (*a*) The dependence of the normal growth rate R on the supersaturation σ. The regions of surface poisoning and two-dimensional nucleation are shown, as deduced from the morphological observation (§3.1). (*b*) The dependence of the step velocity v on the supersaturation σ. The value of the step kinetic coefficient, determined as described in §3.2, is shown.

growth from solutions (Rashkovich & Shekunov, 1990*b*) studied further and interpreted as evidence of the action of two types of impurities (Voronkov & Rashkovich, 1992). The impurity acting at $\sigma \leq 0.4$, after the Cabrera & Vermilyea (1958) stopper mechanism, is strongly absorbed on the crystal surface between steps (terraces) and hinders step motion. With increased supersaturation, the radius of the critical two-dimensional nucleus decreases (Volmer, 1939) and steps are able to pass between the impurity particles. The second impurity decreases the value of the step kinetic coefficient for $0.4 \leq \sigma \leq 0.9$. With increased R, the interval τ, in which terraces between steps are open for impurity adsorption, decreases as (Chernov & Malkin, 1988),

$$\tau = h/R, \tag{7}$$

where h is the step height. The number of adsorbed impurity particles decreases and this leads to a superlinear increase in the step velocity and normal growth rate. When R is sufficiently high, no impurities are adsorbed on the surface and growth kinetics are governed by the properties of pure lysozyme. This enables us for the first time to determine the effective step kinetic coefficient β of a protein substance. From the relation (Chernov, 1984, 1989),

$$\mathrm{v} = \beta \Omega C \sigma, \tag{8}$$

where $\Omega = 2.7 \times 10^{-26}\ \mathrm{m}^3$ is the volume occupied by one lysozyme molecule in the crystal (Steinrauf, 1959), $C = 1.12 \times 10^{24}\ \mathrm{m}^{-3}$ is the molecular concentration of the solution, we get $\beta = (2.8 \pm 0.1) \times 10^{-6}\ \mathrm{m\,s}^{-1}$. The range in the determination of the step kinetic coefficient is determined mainly by the error in the v measurement. This value of β belongs to the temperature interval of linear increase of $\mathrm{v}(\sigma)$, *i.e.* 285–288 K.

It is rather surprising that we have a straight line, determined by the $\mathrm{v}(\sigma)$ at high supersaturations and passing through the origin of the coordinates. The value of the step kinetic coefficient should drop with the increase in supersaturation with falling temperature. (8) should be represented by a curve with negative curvature reflecting the $\beta(T)$ dependence. We investigated this problem by performing experiments described in §3.7. Before this, however, it was necessary to prove and add some more details to the model of impurity influence on protein crystal growth, underlying the determination of the step kinetic coefficient (§§3.3–3.6).

3.3. *Growth kinetics at small supersaturations*

Fig. 9 presents the time dependence of the normal growth rate in the supersaturation region where we assumed a stopper mechanism of impurity action, for two experiments with different preparation. For experiment *A* growth stopped ~7 h after lowering σ and no growth was observed for lower supersaturations. For experiment *B* at the same supersaturation, the growth rate fell gradually until after ~6 h when visible macrosteps appeared. *R* continued to decrease, but somehow more slowly than before. No cessation of growth occurred for 12 h. At a still lower supersaturation of crystal *B* we had a steady growth rate for 10 h. In other experiments, where preparation coincided with that for experiment *B*, neither macrosteps, nor growth cessation was observed at σ as low as 0.25. These facts, together with the morphological observations (§3.1), are evidence that the 'dead zone' at low supersaturations in Fig. 8 is due to an impurity species whose concentration depends on the preparation of the experiment.

3.4. *The influence of the hillock slope*

In experiment *B* measurements were taken on two dislocation-generated step patterns with a different hillock slope (Fig. 7). In accordance with (4), with the smaller p the normal growth rate is smaller (Fig. 10*a*). Step velocity usually (Vekilov *et al.*, 1992*b*; Vekilov & Nanev, 1992) has the reverse dependence on hillock slope due to an interstep concentration field overlap. However, here (Fig. 10*b*) v on the steeper step pattern is higher. This is explicit proof of non-equilibrial impurity influence: the higher hillock slope leads to higher growth rate, smaller times between passing steps [(7)], higher impurity adsorption and, as a result of all these, lower step velocity (Chernov *et al.*, 1986; Chernov & Malkin, 1988).

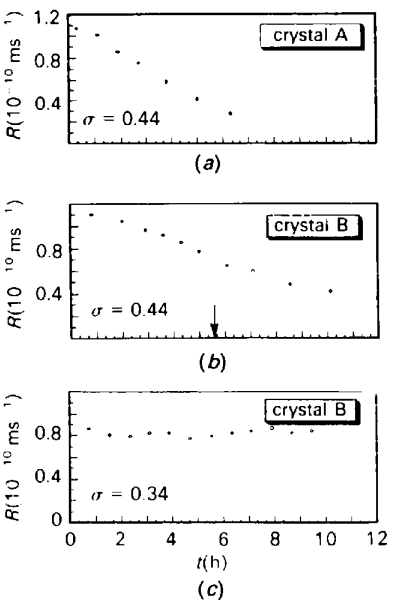

Fig. 9. Time dependencies of the normal growth rate R for crystal *A* (seed washed) and crystal *B* (seed not washed), see §2.1. The supersaturation, at which the measurement was carried out is indicated in each plot. Arrow in (*b*) indicates the time at which macrosteps (Fig. 6) appeared.

3.5. *The effect of higher impurity concentration*

For further evidence of the impurity effect for $0.4 \leq \sigma \leq 1.1$ we carried out one experiment in a solution of nearly the same concentration as before, but with a protein from a different source. We employed lysozyme purchased from Sigma, Inc., often used with or without further purification, in the preceding studies on lysozyme crystal-growth kinetics. The commercial substance is 3× crystallized, without chromatographic, electrophoretic or ultracentrifugal certification of the purity. This product has been electrophoretically proven to contain unidentified protein impurities (Durbin & Feher, 1986; Lorber *et al.*, 1993).

The results for this experiment, denoted as Σ, are shown on Fig. 11. The $R(\sigma)$ relation has the same *S*-like shape as in experiments *A* and *B* (Fig. 8). The *R* values for $0.4 \leq \sigma \leq 1.1$ are approximately 5–6 times lower than in these experiments and they are close to previous measurements in similar conditions (Durbin & Feher, 1986). The $v(\sigma)$ dependence is of the same type as in experiments *A* and *B*. At $\sigma \simeq 1.6$ step velocity reaches the same values as in experiments *A* and *B*. The fact that we have coinciding step velocities at high supersaturations in a solution of different source material and with different impurity concentration supports our supposition that in this region we measure the kinetics of pure lysozyme, without the influence of impurities, and confirms our determination of the step kinetic coefficient. This also means that the kinetic properties of the lysozyme molecules coincide with the two different raw products.

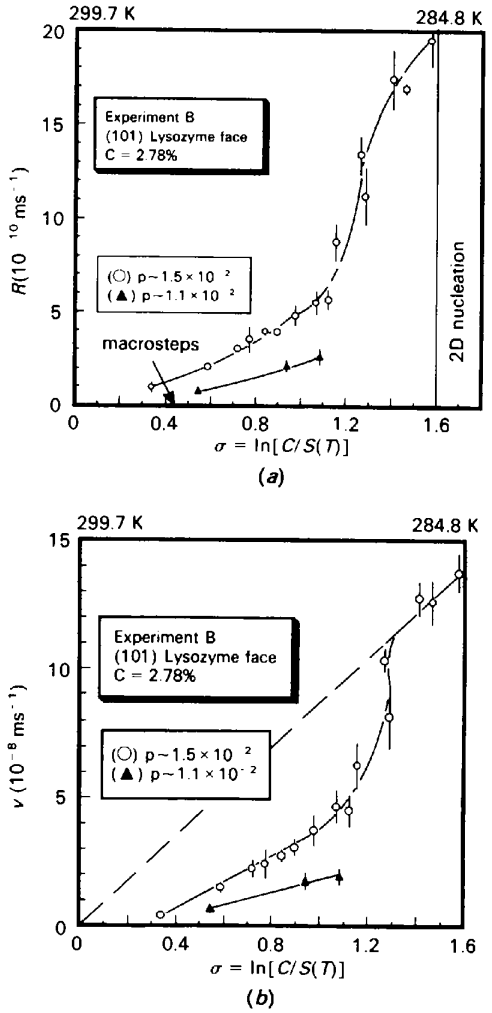

Fig. 10. Kinetic curves for crystal *B* (seed not washed). Different points indicate measurement taken on two step patterns (Fig. 7) with different slope shown in the legend frame. (*a*) Dependence of the normal growth rate *R* on the supersaturation σ. The supersaturation at which macrosteps (Fig. 6) appeared is indicated by an arrow. (*b*) The dependence of the step velocity v on the supersaturation σ. The step kinetic coefficient β coincides with that determined in experiment *A*.

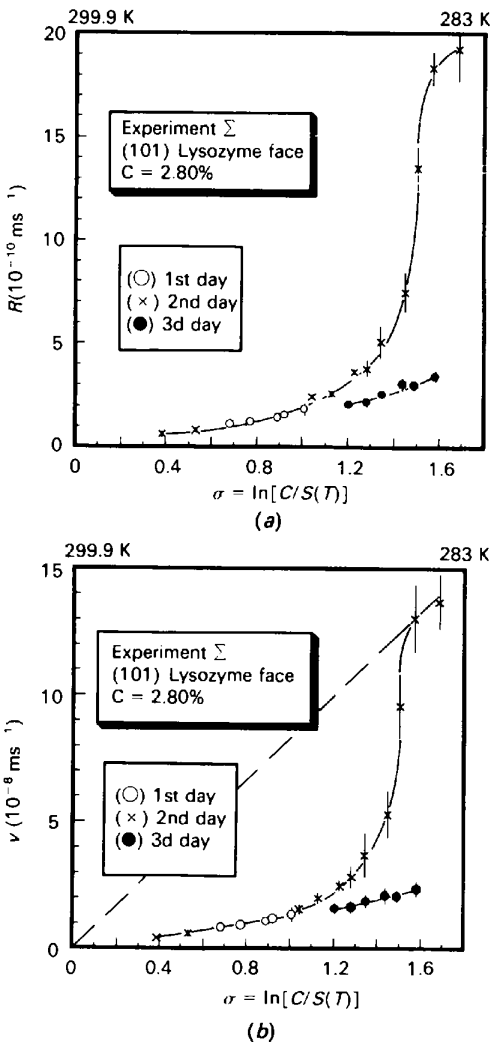

Fig. 11. Kinetic curves for experiment Σ. Different points indicate measurements taken in three successive days after 1 d regeneration. (*a*) The dependence of the normal growth rate *R* on the supersaturation σ. (*b*) The dependence of step velocity v on the supersaturation σ.

The values of v for $0.4 \leq \sigma \leq 1.1$ are much smaller than in *A* and *B* and the region of the non-linear increase moves to higher σ. This result is an unambiguous confirmation of the non-equilibrium impurity influence on lysozyme growth kinetics. Most probably, the impurity species, affecting step motion, is the other protein detected in the commercial Sigma lysozyme (Durbin & Feher, 1986; Lorber *et al.*, 1993). It was also shown recently that the growth rate of an amino acid crystal, a model of proteins, can be greatly reduced as a result of adsorption of a trace amount of additives bearing a structural resemblance (Lechuga-Ballesteros & Rodriguez-Hornedo, 1993).

Another interesting phenomenon, observed in this experiment, is the sharp fall in the kinetic values on the third day of measurements. When supersaturation was lowered to ~1, growth stopped and did not start again at increased supersaturation. Observation of the remaining volume of the solution, kept at room temperature, revealed that the solution became opaque, with an amorphous precipitate on the bottom of the container and with spider's web-like formations floating in the bulk. The solution in the growth cell remained transparent and seemingly unspoilt, presumably because the temperature in the cell during the experiment was lower. It is possible, however, that the same process that spoiled the solution in the container was happening though at a smaller rate, in the growth cell. In experiments *A* and *B* the measurements coincided within 1 week. No visible changes were observed in the solution when kept in a container at room temperature for 2 months.

3.6. *Ageing of the solution*

To check if any changes, influencing growth kinetics, occur to the purer solution, we carried out an experiment with the solution used in *A* and *B* approximately 1 month later. The $v(\sigma)$ plot for that experiment, denoted as *C*, is shown in Fig. 12. The value of the step kinetic coefficient, determined in the 'pure' region $1.2 \leq \sigma \leq 1.6$, $\beta = 2.5 \times 10^{-6}$ m s^{-1} is definitely smaller than in experiments *A* and *B*. One possible reason for this could be a conformational change or partial denaturation of the lysozyme molecules in the solution. The changed lysozyme molecules may act like an impurity of a different type from the ones discussed so far: they do not prevent step motion, but being adsorbed on the steps they decrease the number of active growth sites (kinks) and in this way decrease the step kinetic coefficient (Chernov, 1984; Vekilov & Nanev, 1992). In the impurity-influenced region the values of the step velocity are the same as in experiments *A* and *B*, which could serve as evidence that the impurity acting here is not a form of changed lysozyme.

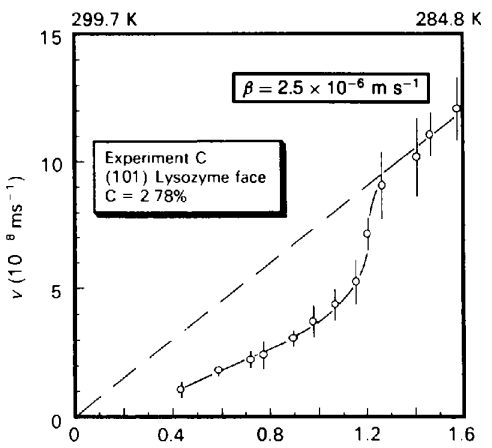

Fig. 12. Step velocity v *versus* supersaturation σ dependence for experiment *C*. The same solution as in *A* and *B*, ~1 month later. The value of the step kinetic coefficient β for this experiment is shown.

3.7. *The effect of temperature*

Fig. 13 presents the dependence of step velocity on supersaturation for experiments *D* and *E*, in which the concentration of the solution was considerably lower than in the experiments reported above. Consequently, the saturation temperature of the solution was lower and the measurements were performed in a lower temperature region. The measured v values are smaller in the whole σ region, but the shape of the curve is preserved. For $\sigma \geq 1.2$ the points lie on a straight line which extrapolates to the origin. Since the molecular concentration of the solution in these experiments is $C = 8.5 \times 10^{23}$ m^{-3}, from (8) we get for the step kinetic coefficient at temperatures 282–286 K, $\beta = (2.8 \pm 0.15) \times 10^{-6}$ m s^{-1}. The step kinetic coefficient does not change with temperature. Recently Boistelle *et al.* (1992) reported an unchanging growth rate in a wide temperature interval (at fixed σ) for one of the forms of α-

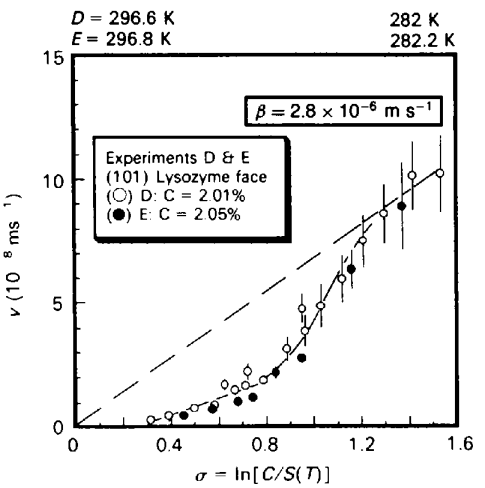

Fig. 13. Step velocity v *versus* supersaturation σ dependence for experiments *D* and *E*. The concentration of the solutions is shown in the label. The temperature ranges of the measurements are indicated on the upper σ axis. The value of the step kinetic coefficient β for this experimental conditions is shown.

amylase isoenzyme crystals, which may reflect the same effect observed by us.

Keeping in mind the error of our measurements and the temperature difference between the two determinations of β ($\Delta T \simeq 3$ K), from the relation (Vekilov *et al.*, 1992*b*),

$$\beta = \beta_0 \exp(-E/RT), \tag{9}$$

(β_0 contains all the factors independent of T) we can estimate the upper limit of the activation energy for step motion E on the (101) lysozyme face: $E \leq 12\,\mathrm{kJ\,mol^{-1}}$. Turning back to §3.2 and Fig. 8(*b*), even if we have the highest possible E value the curve corresponding to (8) with a $\beta(T)$ dependence will be very close to the straight line actually drawn.

The $v(\sigma)$ dependence for an experiment, conducted at a still lower temperature, is shown in Fig. 14. The curve is lower than all the previous ones in the whole supersaturation range. The dead zone at small σ is considerably wider and there is no egress to linearity at high supersaturations. Since adsorption is always exothermic, at lower temperatures impurity adsorption of both kinds of impurities, discussed above, is higher. Moreover, with decreased concentration of the solution, v [see (8)] and R are lower, exposure times of the terraces between steps are greater and the quantity of adsorbed impurity is further increased. These combined effects lead to a wider σ region of action of both impurities and stronger impurity influence on growth.

4. Discussion

We have discussed in a number of examples that kinetic measurements and morphological observations, performed by LMI, can be used to draw valuable information on protein crystal growth. Further, we shall discuss how this knowledge is related to the growth mechanism and to the growth of better protein crystals.

We have presented some strong evidence that when lysozyme crystals grow by dislocation-layer generation, growth is influenced by impurities. The impurity is adsorbed on the terraces between steps on the crystal surface. At higher growth rates, the interval between passing steps gradually becomes shorter than the characteristic adsorption time of the impurity. This leads to non-linear acceleration of growth and, eventually, to growth not influenced by the impurities (§3.2). If the impurities are denatured lysozyme molecules we might expect their number and influence to increase with the time the solution is kept. We saw, however, that impurity-influenced growth rate does not change even after 1 month, although the kinetics of pure lysozyme at higher supersaturations actually changed with time (§3.6). Thus, we conclude that the impurity species, acting at intermediate σ, is most probably some other protein molecule(s), often present in the solution (Weber, 1991; Lorber *et al.*, 1993).

At still higher supersaturations, layer generation by surface two-dimensional (2D) nucleation becomes more intensive than by dislocations and crystal growth proceeds by the 2D nucleation growth mechanism (§3.1). At low supersaturations the surface is sometimes poisoned and growth may even stop due to some different impurities (§§3.1 and 3.3).

Non-linear increase of growth rate of HEW lysozyme in the same region of supersaturation has been observed by several previous authors (Fiddis *et al.*, 1979; Durbin & Feher, 1986; Pusey, 1992). In those cases R was measured as enlargement of a certain face in time. This method is slow, allowing few measurements to be carried out and, especially in the region of dislocation growth, symmetric faces may contribute differently to the enlargement, which leads to inaccuracy. Moreover, no morphological observations were possible simultaneously. In earlier studies it was thought that the non-linear $R(\sigma)$ is due to the surface-nucleation mechanism since the classical dislocation theory predicts a weaker $R(\sigma)$ relation. Our investigation clearly indicates (see Figs. 3, 5 and 7) that at σ up to 1.6 growth layers are generated by dislocations, around which growth hillocks are formed. Further, the non-linear growth was formerly ascribed to increased concentration of clusters of lysozyme molecules at higher supersaturations (Pusey, 1992; Wilson & Pusey, 1992), though no direct experimental evidence was provided. The hypothesis of acceleration due to growth by clusters cannot explain the S-shapes of $R(\sigma)$ and $v(\sigma)$ curves (Fig. 8), the dependence of step velocity on the hillock slope (Fig. 10) and the much lower growth rates and step velocities in the less pure solution (Fig. 11). In the only former investigation on estimated v *versus* σ dependence (Durbin & Feher, 1990), the non-linear increase was supposed to be due to some co-operative effects. In a broader

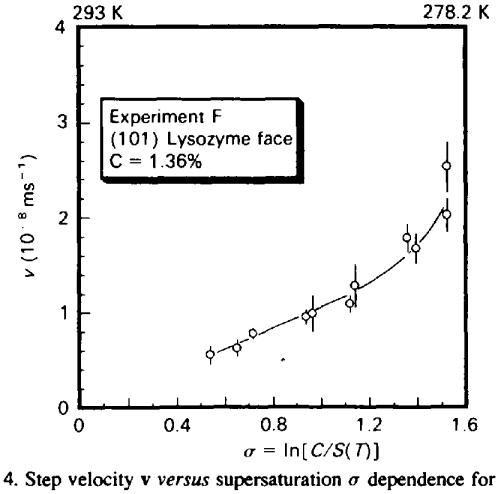

Fig. 14. Step velocity v *versus* supersaturation σ dependence for experiment *F*. The concentration of the solutions is shown in the label. The temperature range of the measurements is indicated on the upper σ axis. Note the expanded scale of the v axis.

sense, the model described above may be considered as a co-operative step motion effect. Now we have added substantial details to the understanding of this step–step interaction.

Our growth experiments were carried out in unstirred solutions, where diffusion transport through the solution may play an important role (Kam *et al.*, 1978). We counterpoised above the kinetic quantities with the bulk supersaturation σ_b, while surface processes actually depend on the surface supersaturation σ_s. In a stagnant solution they are connected by (Chernov, 1984),

$$\sigma_s = \sigma_b[1 + (\beta pr/D)]^{-1}. \quad (10)$$

Here r is the radius of the sphere inscribed in the crystal, for the smallest of our seed crystals $r = 0.35$ mm, $D = 1.03 \times 10^{-10}$ m^2 s^{-1} is the diffusion coefficient of lysozyme in the solution (Mikol *et al.*, 1990). For our system, (10) yields that the surface supersaturation is proportional to the bulk supersaturation and is slightly lower (by ~10%) than it. The diffusion coefficient for lysozyme is only a few times less than for low molecular weight substances, while the kinetic coefficient β is three orders of magnitude smaller. This leads to relatively fast diffusion, followed by slow surface kinetics, which thus becomes the rate-limiting stage. These theoretical considerations are confirmed by the following experimental observations: in different experiments with crystals from 0.7 to 2 mm large [with different r in (10)] and hillock slope in the range 1.1×10^{-2}–1.6×10^{-2} the kinetic measurements coincided under identical conditions. A more definite conclusion requires changing hillock slope in the course of one experiment (Vekilov & Nanev, 1992) or growth measurements in stirred solutions (Vekilov *et al.*, 1992*a*).

The product ΩC in (8) reflects the change of molecular density (molecules per unit volume) upon crystallization. Its value (see §3.2) is $\Omega C = 0.03$. In silver electrocrystallization from a 6 N solution $\Omega C = 0.05$ (Vekilov & Nanev, 1992): the two values are close to each other. Lysozyme growth rate is, however, three orders of magnitude smaller, resulting from the much smaller β. The conclusion here is that the low R characteristic of protein crystals is due to a slow rate of incorporation of solute molecules into steps and not to the solution being very dilute in terms of molecules per unit volume.

This small β value as compared to low molecular weight substances is not a consequence of high activation-energy barriers (§3.7). This should not be surprising. Usually, the activation energy for incorporation into steps is associated with the necessity for solute molecules to shed off their hydration cover before entering the crystal (Burton *et al.*, 1951; Chernov, 1961). This process is not necessary when protein molecules crystallize, since protein crystals contain 30–70wt% water and can be regarded as a very concentrated solution. Therefore, the activation-energy barrier becomes smaller for protein molecules. The main difficulties for entering the steps should then be for entropy reasons. Statistically this could mean that only very few of the protein molecules, approaching an existing growth site on the step, have the correct orientation to be incorporated into the crystal.

Although the activation energy for crystallization of lysozyme is very small, temperature has a strong effect on the growth of the crystals (Fig. 14). Temperature influences protein crystal growth *via* two pathways. At a lower temperature the protein concentration, necessary to keep the same supersaturation, will be lower [(6) and (5)] and this leads to smaller v and R, according to (8). Further, since adsorption is usually exothermic, at a lower temperature the surface concentration of impurities will be higher and their effect on the growth processes stronger.

Growth sometimes stopped at low supersaturations (§§3.1, 3.3). Unlike previous reports (Kam *et al.*, 1978, 1980), when supersaturation was increased, the crystal growth started again; this was repeatedly observed. Therefore, we concluded that this type of growth cessation is due to surface adsorption of impurities and not to accumulation of impurities or other defects in the bulk of the crystal.

Another type of growth cessation occurred when the source material was not of the highest possible purity (§3.5). In the course of measurements, growth rate dropped, then growth stopped and did not restart at any supersaturation. Observing the changes that had occurred in the unused solution, we concluded that the reason for this could be some chemical (or biochemical) reaction between lysozyme and the impurity in the solution resulting, possibly, in a form of denatured or conformationally changed protein. We could not decide whether the new substance is accumulated in the bulk of the crystals or again adsorbed on the terraces between steps. It is difficult to accurately quantify the impurity concentration, but it must be emphasized that our sample is 'pure' from analytical viewpoints. We can say that the growing crystal surface can probably differentiate at least some impurities better than nearly all other analytical techniques.

As to the nucleation event that occurs prior to crystal growth, we are carrying out another series of studies. From an analysis of the concentration decrease in the solution due to the combined effect of nucleation and growth, we have shown that the critical nucleus most probably consists of three or four molecules (Ataka & Asai, 1990; Bessho *et al.*, 1994). Aggregation of lysozyme molecules in precrystalline solutions was also recently studied by small-angle neutron scattering (Nimura *et al.*, 1994). It is probable that the solution from which crystals grow has complex structures. However, we must also point out that there is evidence that the major growth unit is a monomolecular entity (Azuma *et al.*, 1989). Therefore, in the crystal-growth process we

are observing here, the final crystallizing unit is probably a single lysozyme molecule. This also means that the precrystalline aggregates are not likely to be the major 'impurity'.

Based on the above conclusions about the growth processes of protein crystals, we can formulate some recommendations to grow larger and more perfect crystals. The most important recommendation is highest purity. Even scarce amounts of a foreign substance may be adsorbed and accumulated on the growing surface. As shown here, even if pure by most of the modern biochemical analysis methods, the source material may contain impurities which influence crystal growth. On the surface, the impurities make step motion irregular, they produce macrosteps, they may be incorporated into the crystal, and all these lead to point defects, dislocations, inclusions and other unwanted features, decreasing the X-ray diffracting ability of the crystals. Further, it could be worth trying to work at temperatures higher than 277 K (as often used) since at lower temperature the impurity effects are much stronger.

Dislocation growth, in which considerably large portions of the face grow by layers of the same growth hillock, is more regular than growth by two-dimensional nucleation, where for each layer nuclei are formed at different spots. Therefore, it might prove fruitful to grow the crystals at not so high a supersaturation in the dislocation-controlled region. On the other hand, at low supersaturations, growth is powerfully influenced by impurities and so an intermediate supersaturation should be the optimal settlement. These considerations correlate with a result by Ataka & Tanaka (1986) that the largest lysozyme crystals are obtained at concentration to solubility ratio C/S = 2.5–4.0, corresponding to σ = 0.9–1.5 and this is the region where we observed dislocation growth which was not influenced by impurities.

The authors are grateful to the Institute of Physical Chemistry, Sofia, Bulgaria for assistance in the preparation of the experimental set up. One of us (PGV) acknowledges the financial support of the Science and Technology Agency, Government of Japan, for his stay at NIBH.

References

ATAKA, M. & ASAI, M. (1988). *J. Cryst. Growth*, **90**, 86–93.

ATAKA, M. & ASAI, M. (1990). *Biophys. J.* **58**, 807–811.

ATAKA, M. & KATSURA, T. (1992). The Fourth International Conference on Biophysics and Synchrotron Radiation, Tsukuba, Japan. Abstract 354.

ATAKA, M. & TANAKA, S. (1986). *Biopolymers*, **25**, 337–350.

AZUMA, T., TSUKAMOTO, K. & SUNAGAWA, I. (1989). *J. Cryst. Growth*, **98**, 371–376.

BESSHO, Y., ATAKA, M., ASAI, M. & KATSURA, T. (1994). *Biophys. J.* **66**, 310–313.

BOISTELLE, R., ASTIER, J. P., MARCHIS-MOREN, G., DESSEAUX, V. & HASER, R. (1992). *J. Cryst. Growth*, **123**, 109–120.

BURTON, W. K., CABRERA, N. & FRANK, F. C. (1951). *Philos. Trans. R. Soc. London Ser. A*, **243**, 299–358.

CABRERA, N. & VERMILYEA, D. A. (1958). *The Growth of Crystals from Solutions*, in *Growth and Perfection of Crystals*, edited by R. H. DOREMUS, B. W. ROBERTS & D. TURNBULL, pp. 393-408. London: Chapman & Hall.

CARTER, C. W. JR (1990). *Methods: a Companion to Methods in Enzymology*, Vol. 1, pp. 12–24. New York: Oxford Univ. Press.

CARTER, C. W. JR & CARTER, C. W. (1979). *J. Biol. Chem.* **254**, 12219–12223.

CHERNOV, A. A. (1961). *Sov. Phys. Usp.* **4**, 116–148.

CHERNOV, A. A. (1974). *J. Cryst. Growth*, **24/25**, 11–31.

CHERNOV, A. A. (1984). *Modern Crystallography* III: *Growth of Crystals*. Berlin: Springer.

CHERNOV, A. A. (1989). *Contemp. Phys.* **30**, 251–276.

CHERNOV, A. A. & MALKIN, A. J. (1988). *J. Cryst. Growth*, **92**, 432–444.

CHERNOV, A. A., RASHKOVICH, L. N. & MKRTCHAN, A. A. (1986). *J. Cryst. Growth*, **74**, 101–112.

DELUCAS, L. J. & BUGG, C. E. (1987). *Trends Biotechnol.* **5**, 188–193.

DEISENHOFER, J. (1992). The Fourth International Conference on Biophysics and Synchrotron Radiation, Tsukuba, Japan. Abstract, 3.

DURBIN, S. D. & CARLSON, W. E. (1992). *J. Cryst. Growth*, **122**, 71–79.

DURBIN, S. D. & FEHER, G. (1986). *J. Cryst. Growth*, **76**, 583–592.

DURBIN, S.D. & FEHER, G. (1990). *J. Mol. Biol.* **212**, 763–774.

ELGERSMA, A. V., ATAKA, M. & KATSURA, T. (1992). *J. Cryst. Growth*, **122**, 31–40.

FEIGELSON, R. S. (1988). Technical report to NASA, No. NAG8-489.

FIDDIS, R. W., LONGMAN, R. A. & CALVERT, P. D. (1979). *J. Chem. Soc. Faraday Trans.* 1, **75**, 2753–2761.

KAM, Z., SHAIKEVITCH, A., SHORE, H. B. & FEHER, G. (1980). *Electron Microscopy at Molecular Dimensions*, edited by W. BAUMEISTER & W. VOGELL, pp. 302–308. Berlin: Springer.

KAM, Z., SHORE, H. B. & FEHER, G. (1978). *J. Mol. Biol.* **123**, 539–555.

KUZNETSOV, YU. G., CHERNOV, A. A., VEKILOV, P. G. & SMOL'SKII, I. L. (1987). *Soviet Phys. Cryst.* **32**, 584–587.

LECHUGA-BALLESTEROS, D. & RODRIGUEZ-HORNEDO, N. (1993) *J. Colloid Interf. Sci.* **157**, 147–153.

LORBER, B., SKOURI, M., MUNCH, J.-P. & GIEGÉ, R. (1993) *J. Cryst. Growth*, **128**, 1203–1211.

MCPHERSON, A. (1990). *Crystallization of Membrane Proteins*, edited by H. MICHEL, pp. 1–52. Boca Raton: CRC Press.

MCPHERSON, A. (1992). *J. Cryst. Growth*, **122**, 161–167.

MAIWA, K., TSUKAMOTO, K. & SUNAGAWA, I. (1990). *J. Cryst. Growth*, **102**, 43–53.

MALKIN, A. J., CHERNOV, A. A. & ALEXEEV, I. V. (1989). *J. Cryst. Growth*, **97**, 765–769.

MALKIN, A. J., CHEUNG, J. & MCPHERSON, A. (1993). *J. Cryst. Growth*, **126**, 544–554.

MICHEL, H. (1990). Editor. In *Crystallization of Membrane Proteins*. Boca Raton: CRC Press.

MIKOL, V., HIRSCH, E. & GIEGÉ, R. (1990). *J. Mol. Biol.* **213**, 187–195.

NANEV, C. N. & VLADIKOVA, P. (1978). *Electrochim. Acta*, **23**, 325–329.

NIIMURA, N., MINEZAKI, Y., ATAKA, M. & KATSURA, T. (1994) *J. Cryst. Growth*, **137**, 671–675.

PUSEY, M. L. (1992). *J. Cryst. Growth*, **122**, 1–7

RASHKOVICH, L. N. & SHEKUNOV, B. YU. (1990*a*). *J. Cryst. Growth*, **100**, 133–144.

RASHKOVICH, L. N. & SHEKUNOV, B. YU. (1990*b*). *Growth of Crystals*, Vol. 18, edited by E. I. GIVARGIZOV, pp. 124-151. Moscow: Nauka. (In Russian.)

SHAIKEVITCH, A. & KAM, Z. (1981). *Acta Cryst.* A**37**, 871–875.

STEINRAUF, L. K. (1959). *Acta Cryst.* **12**, 77–79.

VAN DER EERDEN, J. P. & MÜLLER-KRUMBHAAR, H. (1986). *Phys. Rev. Lett.* **57**, 2431–2433.

VEKILOV, P. G., ATAKA, M. & KATSURA, T. (1993) *J. Cryst. Growth*, **130**, 317–320.

VEKILOV, P. G., KUZNETSOV, YU. G. & CHERNOV, A. A. (1990). *J. Cryst. Growth*, **102**, 706–716.

VEKILOV, P. G., KUZNETSOV, YU. G. & CHERNOV, A. A. (1992*a*). *J. Cryst. Growth*, **121**, 643–655.

VEKILOV, P. G., KUZNETSOV, YU. G. & CHERNOV, A. A. (1992*b*). *J. Cryst. Growth*, **121**, 44–52.

VEKILOV, P. G. & NANEV, C. (1992). *J. Cryst. Growth*, **125**, 229–236.
VOLMER, M. (1939). *Kinetik der Phasenbildung*. Dresden: Steinkopf.
VORONKOV, V. V. & RASHKOVICH, L. N. (1992). *Kristallografiya*, **37**, 559–570.
WEBER, P. C. (1991). *Advances in Protein Chemistry*, Vol. 41, edited by C. B. ANFINSEN, F. M. RICHARDS, J. T. EDSALL & D. S. EISENBERG, pp. 1–37. San Diego: Academic Press.
WEEKS, J. D. & GILMER, G. H. (1979). *Advan. Chem. Phys.* **40**, 157–228.
WILSON, L. J. & PUSEY, M. L. (1992). *J. Cryst. Growth*, **122**, 8–14.